



Mathematical Analysis of the Role of Heterogeneous Distribution of Excitable and Non-excitable Cells on Early Afterdepolarizations

Seunghyun Kim^{1†} and Daisuke Sato^{2*}

¹ Department of Mathematics, University of California, Davis, Davis, CA, United States, ² Department of Pharmacology, University of California, Davis, Davis, CA, United States

OPEN ACCESS

Edited by:

S. Sridhar,
Robert Bosch Centre for
Cyber-Physical Systems, Indian
Institute of Science, India

Reviewed by:

Fei Geng,
McMaster University, Canada
Alok Ranjan Nayak,
International Institute of Information
Technology, India

*Correspondence:

Daisuke Sato
dsato@ucdavis.edu

† Present Address:

Seunghyun Kim,
Department of Mathematics,
University of California, Los Angeles,
Los Angeles, CA, United States

Specialty section:

This article was submitted to
Biomedical Physics,
a section of the journal
Frontiers in Physics

Received: 16 January 2018

Accepted: 20 September 2018

Published: 12 October 2018

Citation:

Kim S and Sato D (2018)
Mathematical Analysis of the Role
of Heterogeneous Distribution of
Excitable and Non-excitable Cells on
Early Afterdepolarizations.
Front. Phys. 6:117.
doi: 10.3389/fphy.2018.00117

Early afterdepolarizations (EADs) are abnormal oscillations during the plateau phase of the cardiac action potential and have been linked to cardiac arrhythmias. At the cellular level, EADs can be caused by reactivation of the L-type calcium (Ca^{2+}) channels, spontaneous Ca^{2+} releases from the sarcoplasmic reticulum, or both. In tissue, these EADs can trigger action potentials in neighboring cells, which may propagate as a nonlinear wave. In this scenario, EADs are attributed to cellular/subcellular/channel properties. In this study, we show a novel mechanism of EADs due to heterogeneous distribution of excitable and non-excitable cells in tissue, using a physiologically detailed computational model and mathematical analysis. In tissue, excitability of cells depends on the cell type and physiological and pathological conditions. Non-excitable cells create a non-excitable gap in tissue, which has been thought to be a cause of slow waves and reflected waves. Here, we show that the non-excitable gap also can be responsible for EAD generation. However, EADs occur only when the non-excitable gap size is optimal. If the gap size is too small, no EADs occur. If the gap size is too large, the action potential wave cannot propagate through the gap region. We also demonstrate that EADs caused by the non-excitable gap can initiate reentry in tissue, which has been linked to ventricular tachycardia and fibrillation. Thus, the non-excitable gap can lead to both focal and reentrant arrhythmias. EADs shown in this study are spatial phenomena and require tissue heterogeneity. Our study sheds light on the role of tissue heterogeneity on focal and reentrant arrhythmias.

Keywords: early afterdepolarizations, heterogeneity, reflection, excitable media, reentry, arrhythmias, non-excitable gap, cardiac tissue

INTRODUCTION

Sudden cardiac death is one of the major causes of death in the world [1]. Sudden cardiac death is most often caused by arrhythmias. Under normal conditions, action potential waves propagate smoothly in the heart. During arrhythmias, in contrast, action potential waves are less organized and often show spatiotemporally chaotic behaviors. However, it is not clear how regular sinus rhythm becomes irregular arrhythmias.

Cardiac myocytes are excitable cells. These cells are coupled by gap junctions in tissue. The membrane excitability and gap junction coupling are highly heterogeneous in the heart [2, 3]. These heterogeneities are especially amplified under pathological conditions such as heart failure and myocardial infarction [4–9].

Early afterdepolarizations (EADs) are abnormal oscillations of the membrane potential during the plateau phase of the action potential. EADs can be caused by reactivation of the Ca^{2+} and/or Na^{+} channels or spontaneous Ca^{2+} releases from the sarcoplasmic reticulum, or both [10–15]. These abnormal oscillations can re-excite surrounding tissue and cause triggered activities if they overcome the source-sink mismatch [16–20].

Cardiac myocytes are electrotonically coupled via gap junctions in tissue. When some cells are excited in tissue, currents flow from excited cells to neighboring cells via gap junctions and excite the neighboring cells. The propagation excitation forms the action potential wave. Under pathological conditions such as ischemia and myocardial infarction, cells can be less excitable or non-excitable [21, 22]. If one cell is non-excitable, the membrane potential of the cell is passively changed by the membrane potential of surrounding cells. Generally, one or few non-excitable cells do not cause a problem since the action potential wave can pass through these cells. However, as the number of non-excitable cells increases, the action potential wave slows down in this region, and eventually fails to propagate when the number of non-excitable cells exceeds a certain threshold. In addition to propagation failure, non-excitable cells in tissue also can cause retrograde waves, which may lead to focal arrhythmias. This phenomenon is known as “reflection” and shown in experiments using the ventricular tissue, atrial tissue, and Purkinje fiber [23–29]. These reflected waves have been also shown in computer simulations [30–35]. The simplified mathematical model of cardiac tissue showed the mechanisms of reflected waves and the role of the non-excitable region [31]. The detailed analysis using 1- and 2-variable models has shown that the number of reflected waves is highly sensitive to the size of the non-excitable region [33, 35].

In this study, we show how non-excitable cells in excitable tissue affect EAD formation due to reactivation of the Ca^{2+} channels using computational models and mathematical analysis. The key finding in this study is that a small region (1~2 mm) of non-excitable tissue can lead to EADs and promote arrhythmias. Thus, tissue properties are critical for EAD formation as well as cellular properties. Such heterogeneous distribution of non-excitable and excitable cells in tissue, as in pathological conditions such as ischemia, can lead to the onset of ventricular tachycardia and fibrillation.

MATERIALS AND METHODS

Physiological Model

We used a physiologically detailed model of the rabbit ventricular action potential model used in our previous studies [19, 36–38]. The membrane potential is governed by

$$\frac{\partial V(x, t)}{\partial t} = -s(x) \cdot \frac{I_{ion}(x, t)}{C_m} + \nabla \cdot D \nabla V(x, t),$$

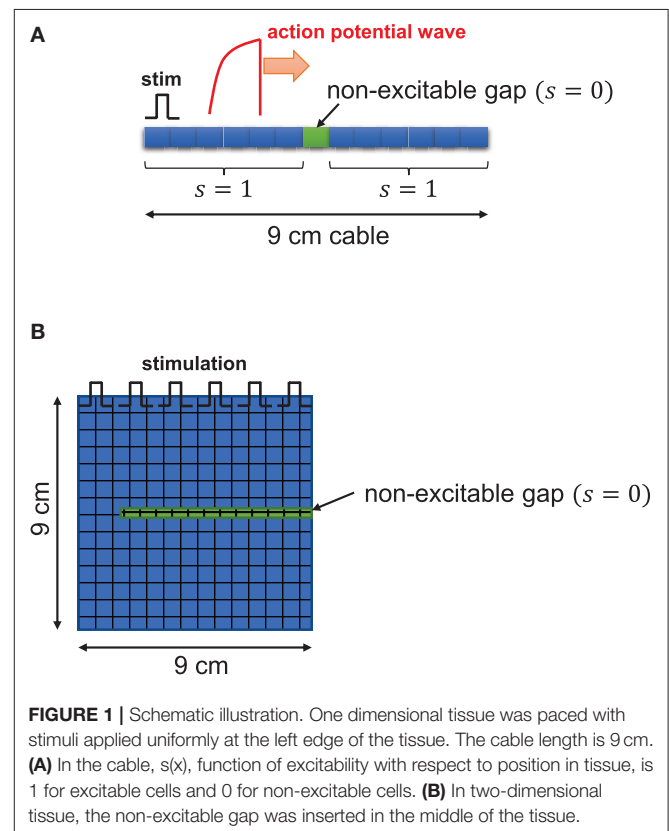
where V is the membrane potential, I_{ion} is the total transmembrane current, C_m is the cell membrane capacitance, D is the effective diffusion constant of the voltage due to currents from neighboring cells through gap junctions, x represents position in space and t is time. In this study, we introduced the variable $s(x)$ to control excitability in tissue as follows (Figure 1A).

$$\begin{cases} s(x) = 0 & \text{for non-excitable cells} \\ s(x) = 1 & \text{for excitable cells} \end{cases}$$

Since the original parameters of this model were built based on the healthy rabbit cell data [37], EADs do not occur even at slow heart rates. In order to promote EAD formation at the cellular level, we modified parameters to reduce repolarization reserve by increasing inward current (I_{CaL}) and reducing K currents. We note that even with these modifications, EADs do not occur without the non-excitable gap. EADs occur only when the non-excitable gap is inserted in tissue and/or repolarization reserve is further reduced by increasing I_{CaL} (or decreasing K current). Parameters and equations used in this study are shown in the **Supplementary Material**.

Computer Simulation

A one-dimensional cable (9 cm) was paced at one end. To ensure propagation, the leftmost five cells were paced in a one-dimensional cable. Non-excitable cells were inserted in the middle of the cable as shown in Figure 1A. The two-dimensional



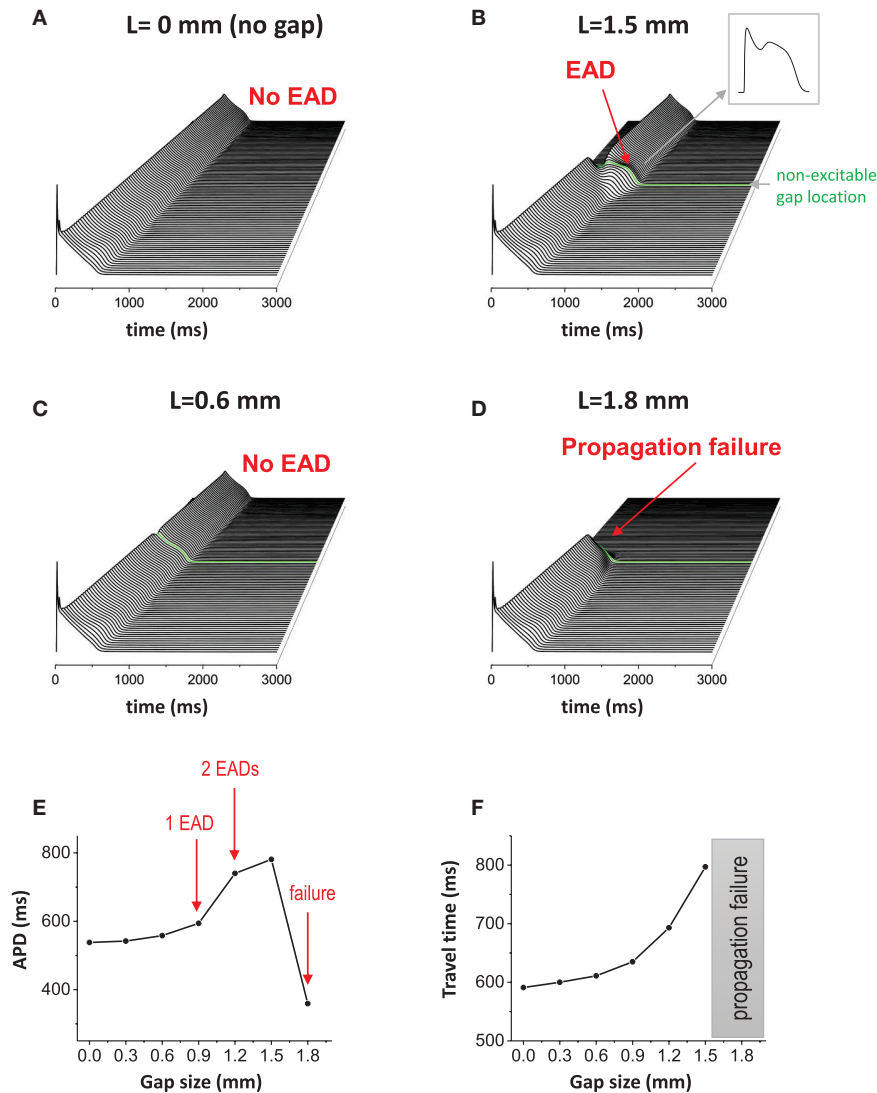


FIGURE 2 | Non-excitable gap causes EADs. **(A)** Without non-excitable gap, the action potential wave propagates without causing EADs in 1D tissue. Space-time plot. **(B)** When non-excitable gap is inserted, EADs occurred around the non-excitable gap region. The maximum APD is 781 ms. The gap size is 1.5 mm. **(C)** If the gap size is too small (0.6 mm), no EADs occurred. **(D)** If the gap size is too large (1.8 mm), propagation failed at the gap region. **(E)** APD vs. the gap size. **(F)** The travel time of action potential wave vs. gap size.

tissue (9×9 cm) was paced from the top and non-excitable cells were inserted as shown in **Figure 1B**. We solve this equation using the operator splitting method [39]. We use the Euler method with the variable time step of $0.01 \sim 0.1$ ms to compute the single cell action potential. The space step (Δx) is $150 \mu\text{m}$, which is similar to the length of the cardiac myocyte. For the numerical accuracy, we used double precision in our simulations and checked the results using smaller time steps. All codes are written in C/C++. We used the 25-node high-performance computing cluster.

Simplified Model

In order to understand the dynamical mechanisms of EADs due to non-excitable gap, we also constructed the reduced

mathematical model of EADs. The basic structure of the model is the same as our previous studies [40]. This model has three variables: membrane voltage (v), and gating variables (f and x). These variables are governed by

$$\begin{aligned} C_m \frac{dv}{dt} &= -(i_{Ca} + i_K) + g_{gap}(v_2 - v), \\ \frac{df}{dt} &= \frac{f_\infty - f}{\tau_f}, \\ \frac{dx}{dt} &= \frac{x_\infty - x}{\tau_x}, \end{aligned}$$

where i_{Ca} is the simplified L-type Ca^{2+} current and i_K is the generic K current, g_{gap} is the effective conductance between

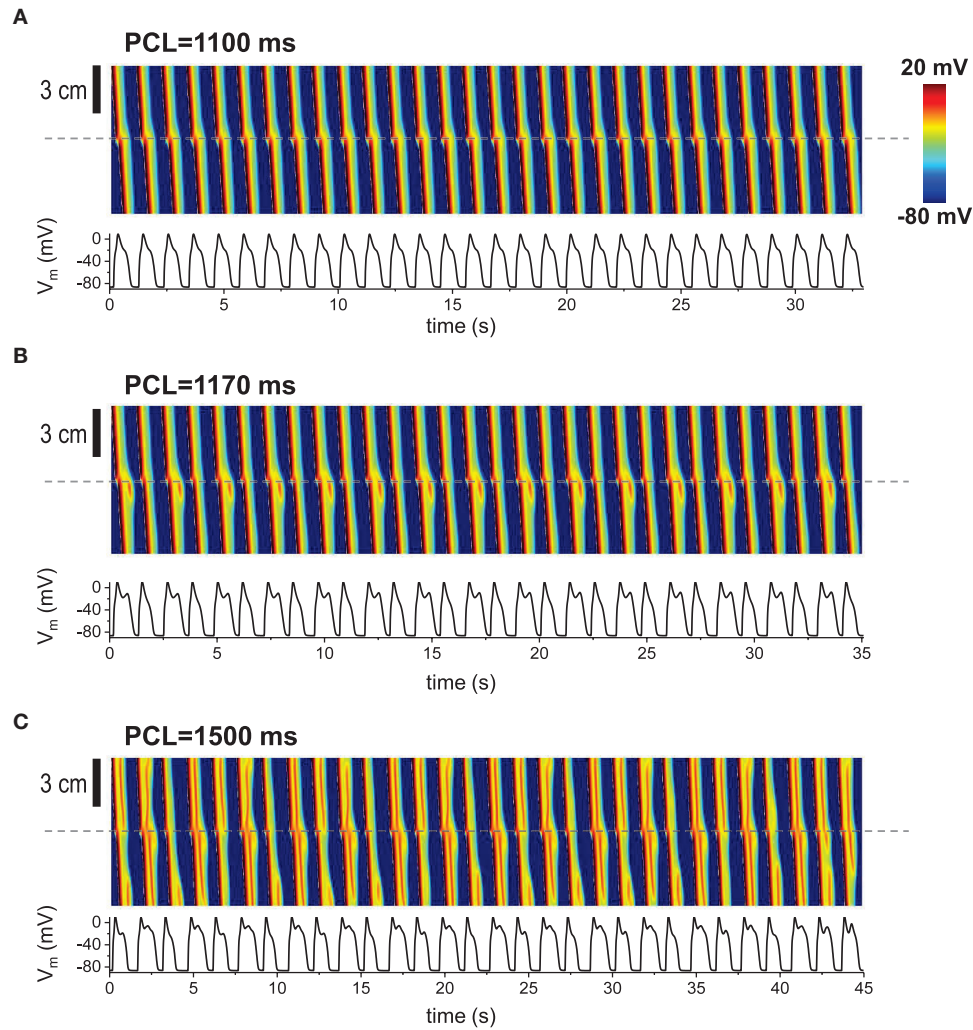


FIGURE 3 | Repetitive pacing When 1D cable was paced repetitively, various patterns appeared. Top: Space-time plot. The AP traces (bottom) were taken at the middle of the cable (indicated by dashed lines). The gap size is 1.5 mm. The tissue was paced 200 times. Last 30 beats are shown here. **(A)** Periodic (period-1) pattern. No EADs at the gap region. **(B)** Period-2. EADs occur every other beat. **(C)** Complex pattern. Spatiotemporal chaos.

proximal and distal regions. v_2 is the membrane potential in the distal region. Due to the large delay at the gap region, the action potential in the distal region remains the plateau phase when the membrane potential in the proximal region is repolarizing. Thus, the membrane potential in the distal region was assumed to be constant. f and x are gating variables of the Ca^{2+} current and the generic K current, respectively. f_∞ and x_∞ are steady state values of f and x gates, respectively. τ_f and τ_x are time constants of f and x gates, respectively. The simplified L-type Ca^{2+} current and the generic K current are

$$\begin{aligned} i_{Ca} &= g_{Ca} d_\infty f (v - e_{Ca}), \\ i_K &= g_k \cdot x \cdot (v - e_k), \end{aligned}$$

where g_{Ca} is the maximum conductance of i_{Ca} , g_k is the maximum conductance of i_k , d_∞ is the instantaneous activation gate of the Ca^{2+} channel, e_{Ca} is the reversal potential of i_{Ca} , e_k is

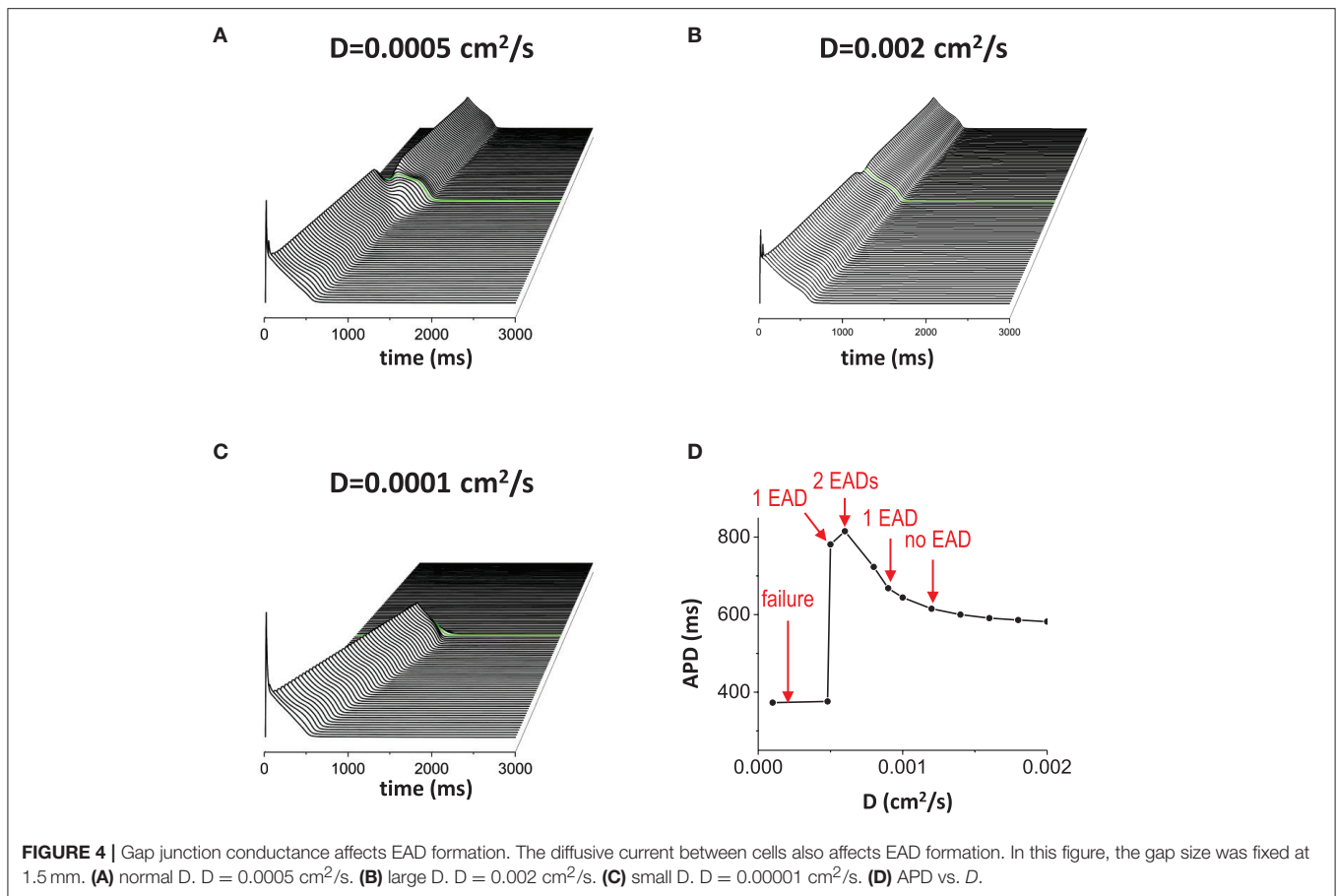
the reversal potential of i_k . Steady state values, d_∞ , f_∞ and x_∞ are voltage dependent and governed by

$$\begin{aligned} d_\infty &= \frac{1}{1 + \exp\left(-\frac{v+32}{6.24}\right)}, \\ f_\infty &= \frac{1}{1 + \exp\left(\frac{v+21}{8.6}\right)}, \\ x_\infty &= \frac{1}{1 + \exp\left(-\frac{v+35}{5}\right)}. \end{aligned}$$

We use the Euler method with the variable time step of 0.1 ms to solve the simplified model.

RESULTS

One-dimensional cable was paced at one end. In this study, the cable length is 9 cm, which is longer than the typical human

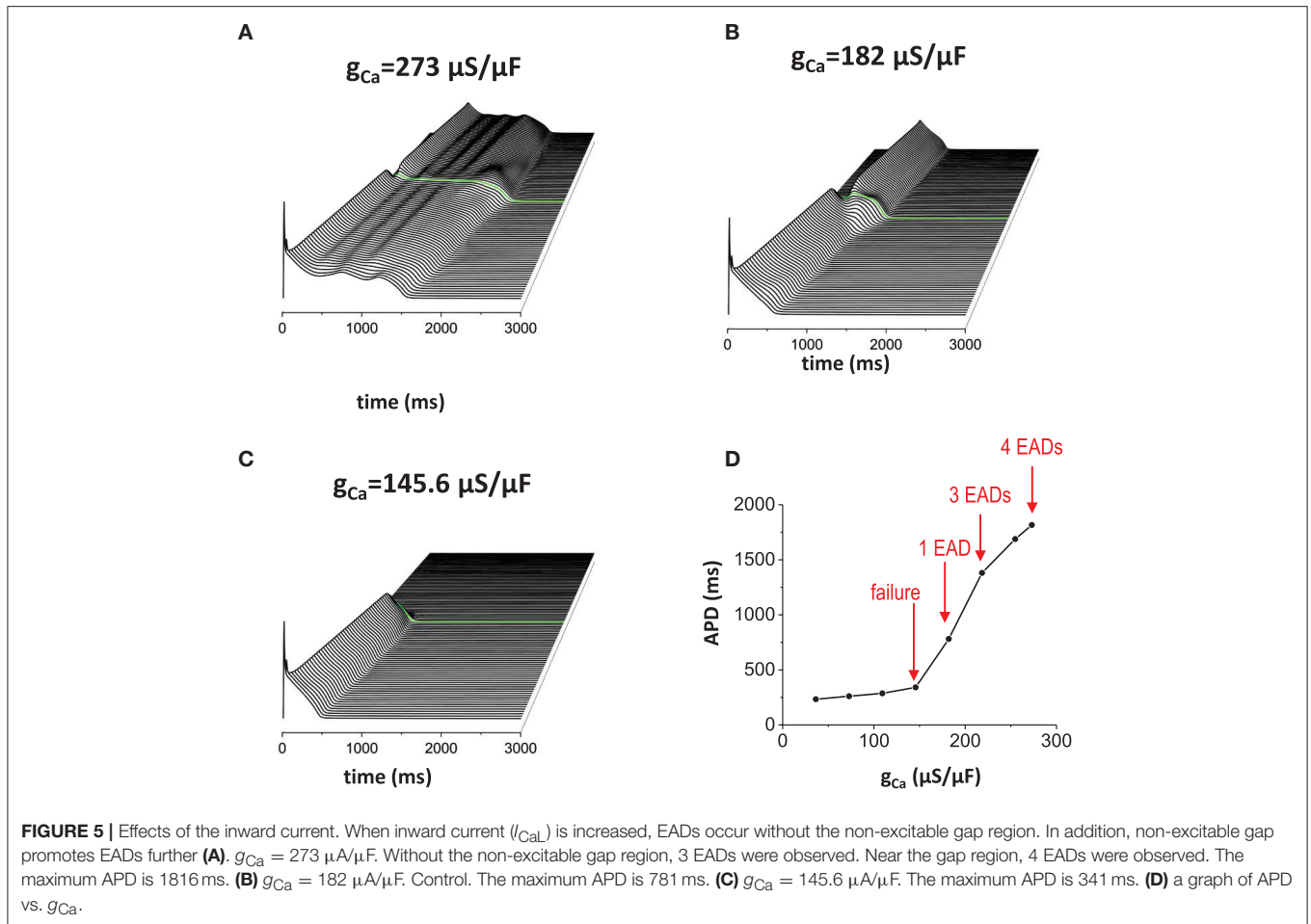


heart size, to avoid unnecessary boundary effects. When cells are well connected via gap junctions without a non-excitable gap, the action potential wave propagates smoothly without EADs in the cable (**Figure 2A**). Hereafter, we refer to this case as the “control” case. The maximum action potential duration (APD) in the cable was 538 ms in the control case. The travel time of the action potential wave from one end to the other end totaling 9 cm was 591 ms. When a non-excitable gap of 1.5 mm (= 10 cells) is inserted in the middle of the cable (**Figures 1, 2B** green line), the propagation speed of the action potential slows down at the gap region. In this case, the travel time of the action potential wave propagated from one end to the other end was 797 ms. Therefore, the delay of the propagation at the gap region is 259 ms. In addition, EADs occur near the gap region (**Figure 2B**). In this case, the maximum APD in the cable was 781 ms. The gap size is critical for the formation of EADs. If the gap size is too small, EADs do not occur (**Figure 2C**). EADs occurred only when the gap size reaches 1.5 mm. On the other hand, if the gap size is too large (gap size greater than or equal to 1.8 mm), the action potential wave cannot propagate due to non-excitability in the gap (**Figure 2D**). **Figure 2E** shows a graph of APD vs. gap size, and the number of EADs with different gap sizes. Additionally, the travel time of action potential wave is depicted against the gap size (**Figure 2F**). Note that the action potential fails to propagate if the gap size is larger than 1.8 mm.

In our previous studies, we have shown that EADs can be periodic and chaotic due to nonlinearity of EAD dynamics [15, 19, 40–42]. When the 1D cable was paced repetitively, various patterns appeared such as periodic (period-1), period-2 and even spatiotemporally chaotic patterns (**Figures 3A–C**). These patterns appear only when non-excitable cells exist in tissue.

When the non-excitable gap exists, changing the gap junction conductance also has the similar effects to the gap size since the effective gap size is proportional to $1/\sqrt{D}$. In other words, the diffusion coefficient D rescales the length of the gap. Thus, although changing the size and changing the gap junction conductance are physiologically different, mathematically, we expect similar results. We used a fixed gap size = 1.5 mm for all simulations in **Figure 4**. When D is normal value ($D = 0.0005 \text{ cm}^2/\text{s}$), 1 EAD was observed near the gap region (**Figure 4A**). If D becomes larger ($D = 0.002 \text{ cm}^2/\text{s}$), the effective gap size becomes smaller and no EADs occurred (**Figure 4B**). If D is too small ($D = 0.00001 \text{ cm}^2/\text{s}$), the action potential wave could not cross the gap region due to the large effective gap (**Figure 4C**). **Figure 4D** shows how diffusive coupling impacts EAD formation. There is an optimal window for EAD formation.

Reducing repolarization reserve by increasing inward currents such as I_{CaL} and/or reducing outward currents such as I_{Kr} and I_{Ks} , promotes EAD generation. When I_{CaL} is increased (**Figure 5A**), APD was prolonged (APD = 1816 ms) and the



action potential wave has EADs without the non-excitable gap. When the non-excitable gap is inserted, it promoted EADs further if the gap size optimal (the gap size is 1.5 mm in **Figure 5**). Near the gap region, four EADs occurred whereas only three EADs occurred in the other regions. **Figure 5B** is the control model for comparison. If the inward current is too small, the action potential is too short to provide enough source current to initiate new action potential in the distal region even if the gap size is optimal for the control model (**Figure 5C**). **Figure 5D** is a graph of APD vs. conductance of the inward current (g_{Ca}), summarizing our observation that EADs occur when the inward current increases.

Reducing outward current also has the same effects (**Figures 6A–D**). When the outward current became smaller (in this case, we reduced I_{NaK}), more EADs occurred (**Figure 6A**). **Figure 6B** is the control model for comparison. Then, when the outward current became too large, the action potential wave failed to propagate (**Figure 6C**). To summarize these results, we plotted a graph of APD against conductance of the outward current (g_{NaK} ; **Figure 6D**).

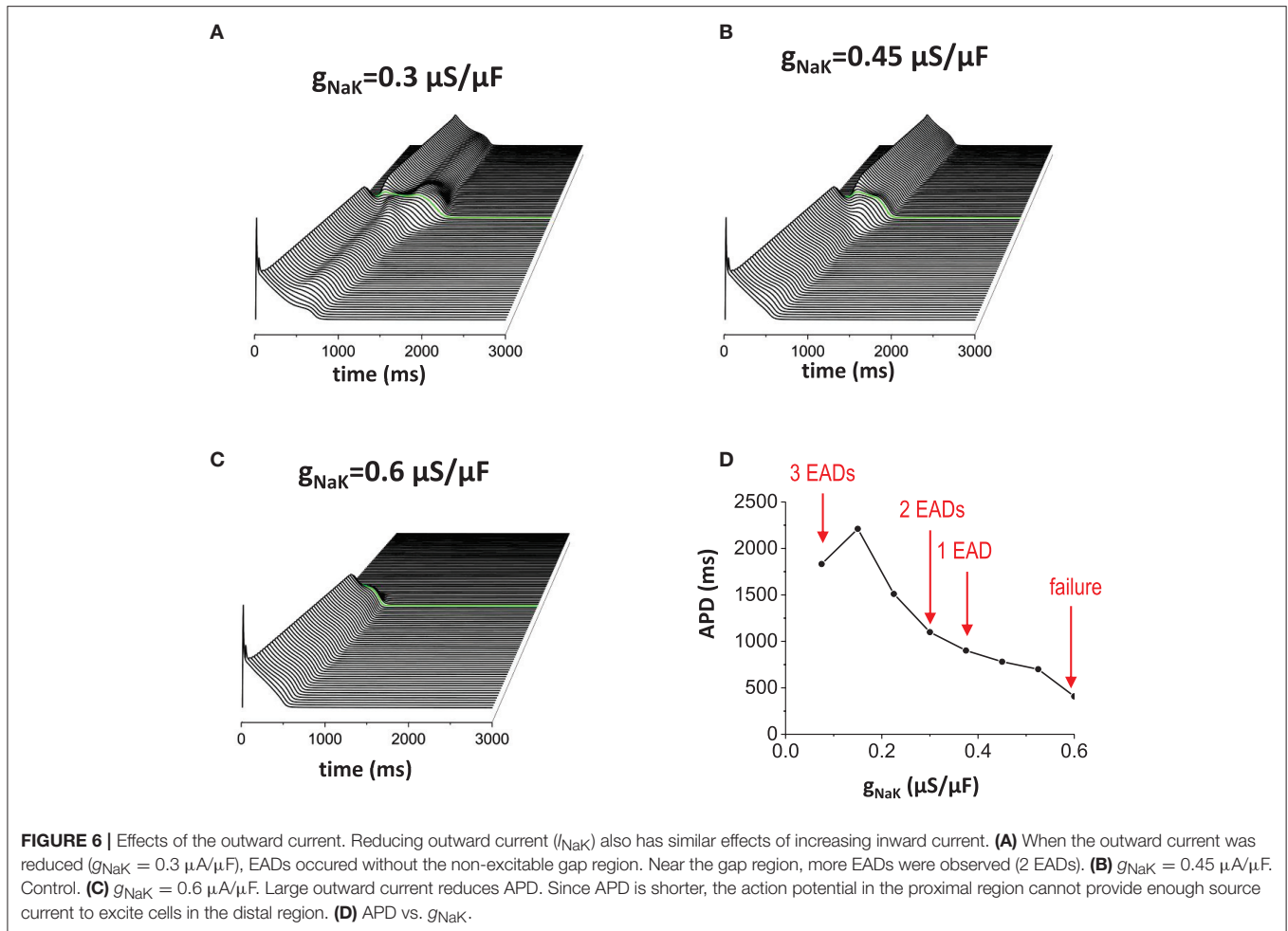
To understand the dynamical mechanisms of EADs due to the non-excitable gap, we analyzed using a simplified mathematical model of EADs (see Material and Methods). In this model, v is

the membrane potential of the cell in the proximal region near the gap. We assessed how current from the distal region promotes EAD generation. We assume the membrane potential of the cell in the distal region (v_2) remains in the plateau phase due to the large delay (>200 ms) of the propagation at the gap region. Since x is the slowest variable in this system, we take it as a parameter. Then, the 2-variable system can be written as

$$\begin{aligned} \frac{dv}{dt} &= F(v, f) = -(g_{Ca}d_{\infty}f(v - e_{Ca}) + g_k \cdot x \cdot (v - e_k)) \\ &\quad + g_{gap}(v_2 - v), \\ \frac{df}{dt} &= G(v, f) = \frac{f_{\infty} - f}{\tau_f}, \end{aligned}$$

where

$$\begin{aligned} d_{\infty} &= \frac{1}{1 + \exp\left(-\frac{v+32}{6.24}\right)}, \\ f_{\infty} &= \frac{1}{1 + \exp\left(\frac{v+21}{8.6}\right)}. \end{aligned}$$



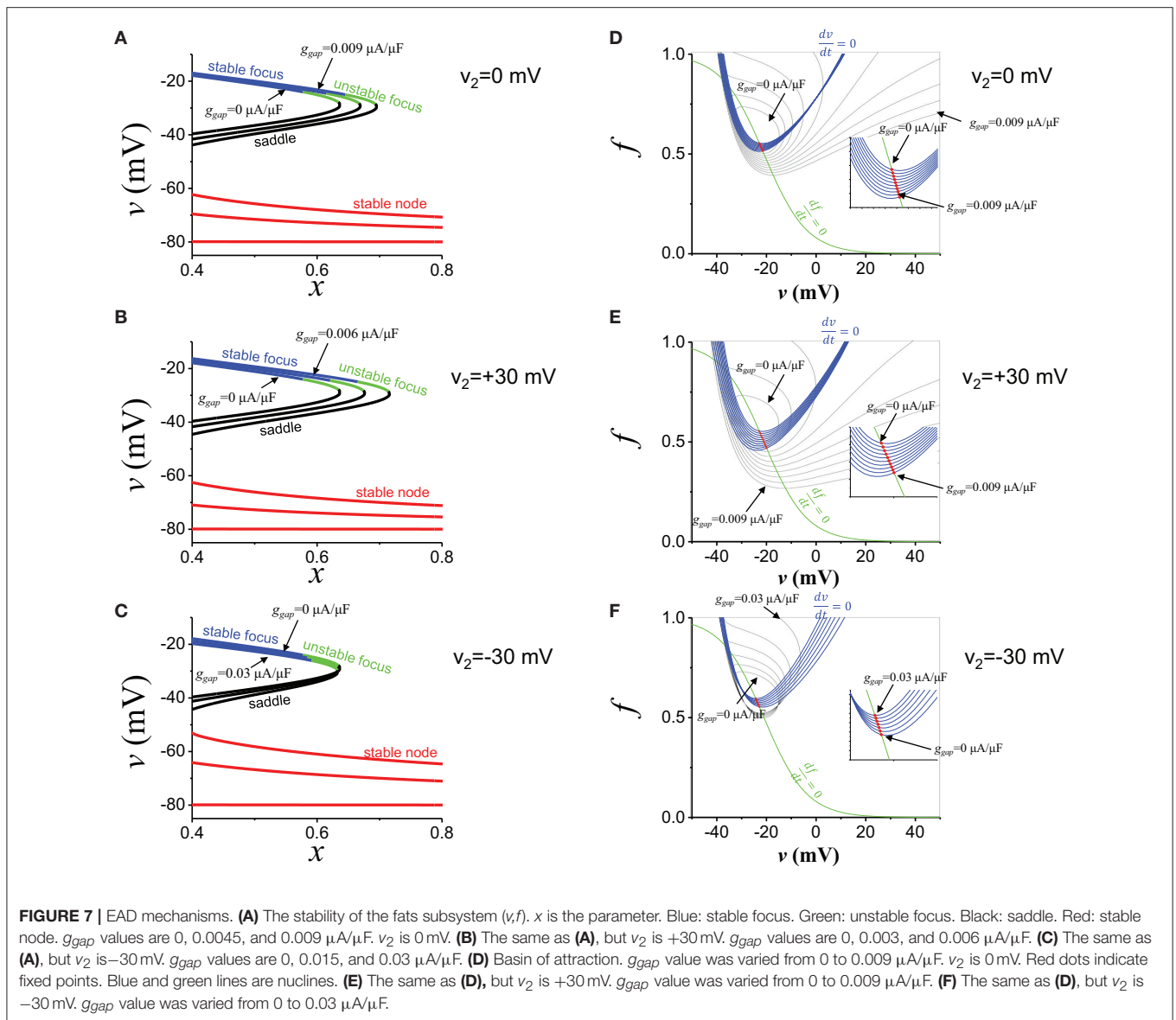
Thus, the matrix to compute the stability of the system is

$$M = \begin{pmatrix} F_v & F_f \\ G_v & G_f \end{pmatrix} = \begin{pmatrix} -g_{Ca}d'_{\infty}fv - g_{Ca}d_{\infty}f - g_kx + g_{gap} & -g_{Ca}d_{\infty}v \\ f'_{\infty}/\tau_f & -1/\tau_f \end{pmatrix}$$

Figures 7A–C show the effects of the current from the distal region. As the gap junction conductance is increased (from $g_{gap}=0$ to $g_{gap}=0.009 \mu A/\mu F$), the attractor region (blue part in **Figure 7A**) was extended and repeller (green part in **Figure 7A**) became attractor (unstable focus \rightarrow stable focus). We varied the distal membrane potential from $+30$ mV to -30 mV (**Figures 7B,C**). In all cases, the current from the distal region promoted oscillatory attractors. We note that if the distal membrane potential becomes lower than ~ -30 mV, the current from the distal region suppresses EADs. We also computed basins of attraction (**Figures 7D–F**). In all cases, the basin of attraction was increased as the gap junction conductance was increased. However, as the distal membrane potential becomes lower, larger conductance was required to extend the basin of attraction (**Figure 7E** vs. **Figure 7F**). On the other hand, the

current from the distal region has little effect on fix points (red dots in **Figure 7**) and EAD oscillations always occur near -20 mV.

When non-excitable cells are inserted in 2-dimensional tissue, EADs caused by the non-excitable gap region can initiate reentry, which has been associated with ventricular tachycardia. Without non-excitable gap, the action potential wave propagates smoothly. When non-excitable gap is inserted (**Figure 1C**), EADs occur near this region. EADs prolong APD. Thus, if cells in this region cannot recover by the time the next wave arrives, the wave cannot propagate in this region. This large dispersion of refractoriness and regional block of the wave can cause reentry (**Figure 8A**, **Supplemental Movie 1**). If the gap size is too small to cause EADs, although there is a small delay of the propagation at the gap region, dispersion of refractoriness is much smaller and rarely causes reentry (**Figure 8B**, **Supplemental Movie 2**). If the gap size is too large, any waves cannot propagate in this region and waves go around this region (**Figure 8C**, **Supplemental Movie 3**). These results demonstrate that non-excitability in tissue can lead to large dispersion of refractoriness and may cause arrhythmias.



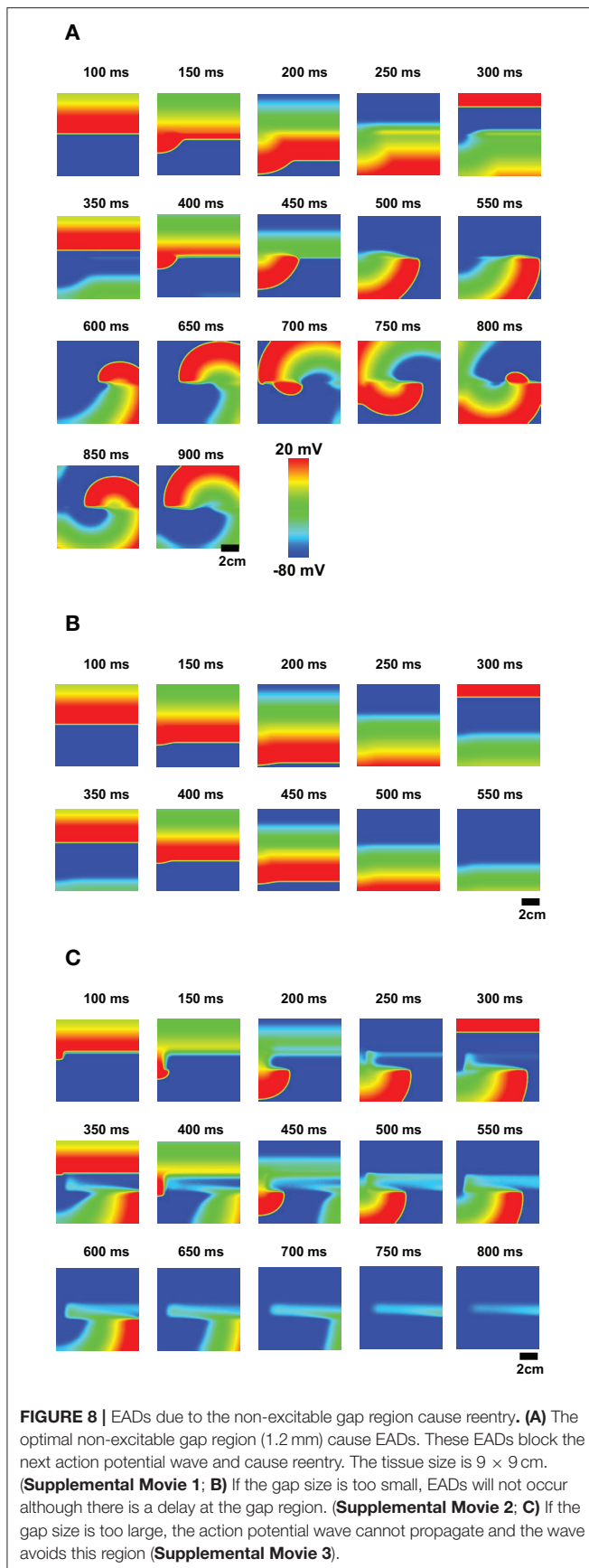
DISCUSSION

Tissue heterogeneity has been thought to be one of the contributing factors of arrhythmias [43–47]. In this study, we investigated how non-excitable cells in excitable tissue promote EADs and thus arrhythmias.

EADs can be caused by reactivation of the Ca^{2+} channels, spontaneous Ca^{2+} releases from the SR, or both [10–15]. In addition, recent studies have shown that reactivation of the Na^+ channels can also lead to EADs [15, 48]. In this study, we showed the mechanism of Ca^{2+} channel-mediated EADs due to heterogeneously distributed excitable and non-excitable cells, and demonstrated reentrant arrhythmias in 2D tissue using physiologically detailed computational models. It has been well-studied how non-excitable cells in excitable tissue can lead to

reflected waves [23–29]. In these studies, the key to the reflected waves was reactivation of the Na^+ channels. In this study, we showed the reflection occurs at the plateau voltage due to reactivation of the Ca^{2+} channels. In our simulations, EADs did not cause a retrograde wave since the amplitude of EADs was too small but prolonged APDs.

The number of EADs is sensitive to the gap size (**Figure 2**). The detailed analysis using a two-variable model has shown that there are infinite patterns of reflected waves (1 reflected wave, 2 reflected waves, 3 reflected waves ... infinite reflected waves) between normal propagation (no reflected waves) and propagation failure when the gap size is varied [33]. In our study, we did not observe these patterns even when the gap size is finely tuned. This is probably because the memory effect in the model interfered the patterns.



In tissue, large dispersion of refractoriness can initiate reentry [49]. When non-excitable cells are inserted in 2D tissue, dispersion of refractoriness can be observed without EADs (**Figure 8B**, **Supplemental Movie 2**). However, the dispersion is small in this case. When EADs occur, the dispersion becomes large enough to initiate reentry (**Figure 8A**, **Supplemental Movie 1**). The non-excitable gap also becomes an anchor of the spiral waves (**Supplemental Movie 1**). But no EADs were observed since the cycle of the rotation of the spiral wave was too fast for EADs. If the gap size is too large, the gap region blocks action potential waves (**Figure 8C**, **Supplemental Movie 3**). It is known that obstacles in tissue can lead to reentry [50, 51]. Thus, the large gap region can also initiate reentry by different mechanisms.

It is known that tissue geometry is also an important factor for reflected waves [32]. When an action potential wave propagates from a narrow path to a wide path, the propagation speed slows down due to the source-sink mismatch. This delay can re-excite the cells in the narrow path and cause a retrograde wave. Thus, propagation delay due to tissue geometry may be able to initiate EADs. This possibility needs to be investigated.

Reflected waves have been observed and investigated in various systems such as cardiac tissue and neurons. The cardiac subcellular Ca^{2+} system is also an excitable system. Under normal conditions, Ca^{2+} release from the sarcoplasmic reticulum (SR) forms a spark. However, when Ca^{2+} sparks recruit new Ca^{2+} sparks in neighboring Ca^{2+} release units, Ca^{2+} sparks propagate as a wave [52, 53]. Each Ca^{2+} release unit contains a few to several hundred ryanodine receptors [54–58] and the number of ryanodine receptors affects the positive feedback process known as Ca^{2+} -induced Ca^{2+} release [58, 59]. In addition, the subcellular structure is very complex. These subcellular heterogeneities may lead to reflection and form complex patterns in Ca^{2+} waves.

In this paper, we showed only mathematical and computational results. These results should be verified in experiments. Reflected waves have been observed in many wet experiments. We expect that we can use the same experimental setup for EADs due to non-excitable cells. However, to observe EADs, repolarization reserve needs to be reduced.

CONCLUSIONS

Cellular mechanisms of EADs have been widely studied. In this study, we showed that tissue properties are also critical for initiation and promotion of EADs. Non-excitable gap in tissue can promote EADs and prolonged action potentials due to EADs can cause conduction block and reentry of the action potential wave.

The limitation of this study is that we considered only Ca^{2+} channel reactivation. Retrograde waves propagate when the Na^+ channels are reactivated. If both cases are considered, focal and reentrant arrhythmias can coexist and the dynamics will become much more complex.

Ablation creates non-excitable tissue. The border zone of myocardial infarction is also mixture of

excitable and non-excitabile cells. Our study implies that EADs can be promoted in these regions due to tissue heterogeneity. This study sheds light on the role of tissue heterogeneity on EAD generation and initiation of reentrant arrhythmias.

AUTHOR CONTRIBUTIONS

All authors SK and DS contributed ideas and discussion. All authors performed computer simulations and mathematical analysis, wrote the manuscript, approved the final version of the manuscript and agree to be accountable for all aspects of the work.

FUNDING

This work was supported by National Institutes of Health grant R00-HL111334, American Heart Association Grant-in-Aid

16GRNT31300018, and Amazon AWS Cloud Credits for Research (DS).

ACKNOWLEDGMENTS

The authors wish to thank Dr. Timothy J. Lewis for a critical reading of the manuscript, and his comments and suggestions.

SUPPLEMENTARY MATERIAL

The Supplementary Material for this article can be found online at: <https://www.frontiersin.org/articles/10.3389/fphy.2018.00117/full#supplementary-material>

Supplemental Movie 1 | Movie of **Figure 8A**.

Supplemental Movie 2 | Movie of **Figure 8B**.

Supplemental Movie 3 | Movie of **Figure 8C**.

REFERENCES

- Zipes DP, Wellens HJJ. Sudden cardiac death. *Circulation* (1998) **98**:2334–51.
- Roberts-Thomson KC, Lau DH, Sanders P. The diagnosis and management of ventricular arrhythmias. *Nat Rev Cardiol.* (2011) **8**:311–21. doi: 10.1038/nrcardio.2011.15
- Burchfield JS, Xie M, Hill JA. Pathological ventricular remodeling: mechanisms: part 1 of 2. *Circulation* (2013) **128**:388–400. doi: 10.1161/circulationaha.113.001878
- Peters NS. Myocardial gap junction organization in ischemia and infarction. *Microsc Res Tech.* (1995) **31**:375–86. doi: 10.1002/jemt.1070310507
- Saffitz JE, Schuessler RB, Yamada KA. Mechanisms of remodeling of gap junction distributions and the development of anatomic substrates of arrhythmias. *Cardiovasc Res.* (1999) **42**:309–17.
- Jongsma HJ, Wilders R. Gap junctions in cardiovascular disease. *Circ Res.* (2000) **86**:1193–7. doi: 10.1161/01.RES.86.12.1193
- Severs NJ. Gap junction remodeling in heart failure. *J Card Fail* (2002) **8**:S293–9. doi: 10.1054/jcaf.2002.129255
- Severs NJ, Coppen SR, Dupont E, Yeh HI, Ko YS, Matsushita T. Gap junction alterations in human cardiac disease. *Cardiovasc Res.* (2004) **62**:368–77. doi: 10.1016/j.cardiores.2003.12.007
- Bruce AF, Rothery S, Dupont E, Severs NJ. Gap junction remodelling in human heart failure is associated with increased interaction of connexin43 with ZO-1. *Cardiovas Res.* (2008) **77**:757–65. doi: 10.1093/cvr/cvm083
- January C, Riddle J. Early afterdepolarizations: mechanism of induction and block. A role for L-type Ca²⁺ current. *Circ Res.* (1989) **64**:977–90.
- January CT, Moscucci A. Cellular mechanisms of early afterdepolarizations. *Ann N Y Acad Sci.* (1992) **644**:23–32. doi: 10.1111/j.1749-6632.1992.tb30999.x
- Zeng J, Rudy Y. Early afterdepolarizations in cardiac myocytes: mechanism and rate dependence. *Biophys J.* (1995) **68**:949–64. doi: 10.1016/s0006-3495(95)80271-7
- Viswanathan PC, Rudy Y. Pause induced early afterdepolarizations in the long QT syndrome: a simulation study. *Cardiovas Res.* (1999) **42**:530–42. doi: 10.1016/s0008-6363(99)00035-8
- Volders PGA, Vos MA, Szabo B, Sipido KR, de Groot SHM, Gorgels APM, et al. Progress in the understanding of cardiac early afterdepolarizations and torsades de pointes: time to revise current concepts. *Cardiovas Res.* (2000) **46**:376–92. doi: 10.1016/s0008-6363(00)00022-5
- Sato D, Clancy CE, Bers DM. Dynamics of sodium current mediated early afterdepolarizations. *Heliyon* (2017) **3**:e00388. doi: 10.1016/j.heliyon.2017.e00388
- Gilmour RF, Moise S. Triggered activity as a mechanism for inherited ventricular arrhythmias in German shepherd dogs. *J Am Coll Cardiol.* (1996) **27**:1526–33. doi: 10.1016/0735-1097(95)00618-4
- Burashnikov A, Antzelevitch C. Reinduction of atrial fibrillation immediately after termination of the arrhythmia is mediated by late phase 3 early afterdepolarization-induced triggered activity. *Circulation* (2003) **107**:2355–60. doi: 10.1161/01.cir.0000065578.00869.7c
- Patterson E, Jackman WM, Beckman KJ, Lazzara R, Lockwood D, Scherlag BJ, et al. Spontaneous pulmonary vein firing in man: relationship to tachycardia-pause early afterdepolarizations and triggered arrhythmia in canine pulmonary veins *in vitro*. *J Cardiovas Electrophysiol.* (2007) **18**:1067–75. doi: 10.1111/j.1540-8167.2007.00909.x
- Sato D, Xie LH, Sovari AA, Tran DX, Morita N, Xie F, et al. Synchronization of chaotic early afterdepolarizations in the genesis of cardiac arrhythmias. *Proc Natl Acad Sci USA.* (2009) **106**:2983–8. doi: 10.1073/pnas.0809148106
- Xie Y, Sato D, Garfinkel A, Qu Z, Weiss JN. So little source, so much sink: requirements for afterdepolarizations to propagate in tissue. *Biophys J.* (2010) **99**:1408–15. doi: 10.1016/j.bpj.2010.06.042
- Janse MJ, Wit AL. Electrophysiological mechanisms of ventricular arrhythmias resulting from myocardial ischemia and infarction. *Physiol Rev.* (1989) **69**:1049–169. doi: 10.1152/physrev.1989.69.4.1049
- Rodríguez B, Trayanova N, Noble D. Modeling cardiac ischemia. *Ann N Y Acad Sci.* (2006) **1080**:395–414. doi: 10.1196/annals.1380.029
- Antzelevitch C, Jalife J, Moe GK. Characteristics of reflection as a mechanism of reentrant arrhythmias and its relationship to parasystole. *Circulation* (1980) **61**:182–91.
- Antzelevitch C, Moe GK. Electrotonically mediated delayed conduction and reentry in relation to “slow responses” in mammalian ventricular conducting tissue. *Circ Res.* (1981) **49**:1129–39.
- Jalife J, Moe GK. Excitation, conduction, and reflection of impulses in isolated bovine and serum cardiac purkinje fibers. *Circ Res.* (1981) **49**:233–47.
- Antzelevitch C, Bernstein MJ, Feldman HN, Moe GK. Parasystole, reentry, and tachycardia: a canine preparation of cardiac arrhythmias occurring across inexcitable segments of tissue. *Circulation* (1983) **68**:1101–15.
- Rozanski GJ, Jalife J, Moe GK. Reflected reentry in nonhomogeneous ventricular muscle as a mechanism of cardiac arrhythmias. *Circulation* (1984) **69**:163–73.
- Lukas A, Antzelevitch C. Reflected reentry, delayed conduction, and electrotonic inhibition in segmentally depressed atrial tissues. *Can J Physiol Pharmacol.* (1989) **67**:757–64.
- Auerbach DS, Grz?da KR, Furspan PB, Sato PY, Mironov S, Jalife J. Structural heterogeneity promotes triggered activity, reflection and

- arrhythmogenesis in cardiomyocyte monolayers. *J Physiol.* (2011) **589**:2363–81. doi: 10.1113/jphysiol.2010.200576
30. Goldstein SS, Rall W. Changes of action potential shape and velocity for changing core conductor geometry. *Biophys J.* (1974) **14**:731–57. doi: 10.1016/s0006-3495(74)85947-3
 31. Cabo C, Barr RC. Reflection after delayed excitation in a computer model of a single fiber. *Circ Res.* (1992) **71**:260–70.
 32. Zhou Y, Bell J. Study of propagation along nonuniform excitable fibers. *Math Biosci.* (1994) **119**:169–203.
 33. Lewis TJ. *The Effects of Nonexcitable Regions on Signal Propagation in Excitable Media: Propagation Failure and Reflection.* Ph.D. Thesis, University of Utah, Salt Lake City, UT (1998).
 34. Keener JP, Lewis TJ. Wave-block in excitable media due to regions of depressed excitability. *SIAM J Appl Math.* (2000) **61**:293–316. doi: 10.1137/s0036139998349298
 35. Cyttrynbaum EN, Lewis TJ. A global bifurcation and the appearance of a one-dimensional spiral wave in excitable media. *SIAM J Appl Dynam Syst.* (2009) **8**:348–70. doi: 10.1137/080722254
 36. Mahajan A, Sato D, Shiferaw Y, Baher A, Xie LH, Peralta R, et al. Modifying L-type calcium current kinetics: consequences for cardiac excitation and arrhythmia dynamics. *Biophys J.* (2008) **94**:411–23. doi: 10.1529/biophysj.106.98590
 37. Mahajan A, Shiferaw Y, Sato D, Baher A, Olcese R, Xie LH, et al. A rabbit ventricular action potential model replicating cardiac dynamics at rapid heart rates. *Biophys J.* (2008) **94**:392–410. doi: 10.1529/biophysj.106.98160
 38. Xie Y, Grandi E, Bers DM, Sato D. How does beta-adrenergic signalling affect the transitions from ventricular tachycardia to ventricular fibrillation? *Europace* (2014) **16**:452–7. doi: 10.1093/europace/eut412
 39. Qu Z, Garfinkel A. An advanced algorithm for solving partial differential equation in cardiac conduction. *IEEE Trans Biomed Eng.* (1999) **46**:1166–8.
 40. Xie Y, Izu LT, Bers DM, Sato D. Arrhythmogenic transient dynamics in cardiac myocytes. *Biophys J.* (2014) **106**:1391–7. doi: 10.1016/j.bpj.2013.12.050
 41. Tran DX, Sato D, Yochelis A, Weiss JN, Garfinkel A, Qu Z. Bifurcation and chaos in a model of cardiac early afterdepolarizations. *Phys Rev Lett.* (2009) **102**:258103. doi: 10.1103/PhysRevLett.102.258103
 42. Sato D, Xie LH, Nguyen TP, Weiss JN, Qu Z. Irregularly appearing early afterdepolarizations in cardiac myocytes: random fluctuations or dynamical chaos? *Biophys J.* (2010) **99**:765–73. doi: 10.1016/j.bpj.2010.05.019
 43. Schmidt A, Azevedo CF, Cheng A, Gupta SN, Bluemke DA, Foo TK, et al. Infarct tissue heterogeneity by magnetic resonance imaging identifies enhanced cardiac arrhythmia susceptibility in patients with left ventricular dysfunction. *Circulation* (2007) **115**:2006–14. doi: 10.1161/circulationaha.106.653568
 44. Bishop MJ, Connolly A, Plank G. Structural heterogeneity modulates effective refractory period: a mechanism of focal arrhythmia initiation. *PLoS ONE* (2014) **9**:e109754. doi: 10.1371/journal.pone.0109754
 45. Qu Z, Weiss JN. Mechanisms of ventricular arrhythmias: from molecular fluctuations to electrical turbulence. *Annu Rev Physiol.* (2015) **77**:29–55. doi: 10.1146/annurev-physiol-021014-071622
 46. Kazbanov IV, ten Tusscher KH, Panfilov AV. Effects of heterogeneous diffuse fibrosis on arrhythmia dynamics and mechanism. *Sci Rep.* (2016) **6**:20835. doi: 10.1038/srep20835
 47. Varela M, Colman MA, Hancox JC, Aslanidi OV. Atrial heterogeneity generates re-entrant substrate during atrial fibrillation and anti-arrhythmic drug action: mechanistic insights from canine atrial models. *PLoS Comput Biol.* (2016) **12**:e1005245. doi: 10.1371/journal.pcbi.1005245
 48. Edwards AG, Grandi E, Hake JE, Patel S, Li P, Miyamoto S, et al. Nonequilibrium reactivation of Na⁺ current drives early afterdepolarizations in mouse ventricle. *Circ Arrhythm Electrophysiol.* (2014) **7**:1205–13. doi: 10.1161/circep.113.001666
 49. Weiss JN, Karma A, Shiferaw Y, Chen PS, Garfinkel A, Qu Z. From pulsus to pulseless: the saga of cardiac alternans. *Circ Res.* (2006) **98**:1244–53. doi: 10.1161/01.RES.0000224540.97431.f0
 50. Panfilov AV, Keener JP. Effects of high frequency stimulation on cardiac tissue with an inexcitable obstacle. *J Theor Biol.* (1993) **163**:439–48. doi: 10.1006/jtbi.1993.1129
 51. Spector PS, Habel N, Sobel BE, Bates JH. Emergence of complex behavior: an interactive model of cardiac excitation provides a powerful tool for understanding electric propagation. *Circ Arrhythm Electrophysiol.* (2011) **4**:586–91. doi: 10.1161/circep.110.961524
 52. Dawson SP, Keizer J, Pearson JE. Fire-diffuse-fire model of dynamics of intracellular calcium waves. *Proc Natl Acad Sci USA.* (1999) **96**:6060–3.
 53. Izu LT, Wier WG, Balke CW. Evolution of cardiac calcium waves from stochastic calcium sparks. *Biophys J.* (2001) **80**:103–20. doi: 10.1016/s0006-3495(01)75998-x
 54. Franzini-Armstrong C, Protasi F, Ramesh V. Shape, size, and distribution of Ca²⁺ release units and couplons in skeletal and cardiac muscles. *Biophys J.* (1999) **77**:1528–39. doi: 10.1016/S0006-3495(99)77000-1
 55. Soeller C, Crossman D, Gilbert R, Cannell MB. Analysis of ryanodine receptor clusters in rat and human cardiac myocytes. *Proc Natl Acad Sci. USA.* (2007) **104**:14958–63. doi: 10.1073/pnas.0703016104
 56. Baddeley D, Jayasinghe ID, Lam L, Rossberger S, Cannell MB, Soeller C. Optical single-channel resolution imaging of the ryanodine receptor distribution in rat cardiac myocytes. *Proc Natl Acad Sci. USA.* (2009) **106**:22275–80. doi: 10.1073/pnas.0908971106
 57. Soeller C, Jayasinghe ID, Li P, Holden AV, Cannell MB. Three-dimensional high-resolution imaging of cardiac proteins to construct models of intracellular Ca²⁺ signalling in rat ventricular myocytes. *Exp Physiol.* (2009) **94**:496–508. doi: 10.1113/expphysiol.2008.043976
 58. Galice S, Xie Y, Yang Y, Sato D, Bers DM. Size matters: ryanodine receptor cluster size affects arrhythmogenic sarcoplasmic reticulum calcium release. *J Am Heart Assoc.* (2018) **7**:e008724. doi: 10.1161/jaha.118.008724
 59. Sobie EA, Dilly KW, dos Santos Cruz J, Lederer WJ, Jafri MS. Termination of cardiac Ca(2+) sparks: an investigative mathematical model of calcium-induced calcium release. *Biophys J.* (2002) **83**:59–78. doi: 10.1016/S0006-3495(02)75149-7

Conflict of Interest Statement: The authors declare that the research was conducted in the absence of any commercial or financial relationships that could be construed as a potential conflict of interest.

Copyright © 2018 Kim and Sato. This is an open-access article distributed under the terms of the Creative Commons Attribution License (CC BY). The use, distribution or reproduction in other forums is permitted, provided the original author(s) and the copyright owner(s) are credited and that the original publication in this journal is cited, in accordance with accepted academic practice. No use, distribution or reproduction is permitted which does not comply with these terms.